Mechanistic Study of HCV Polymerase Inhibitors at Individual Steps of the Polymerization Reaction

Yaya Liu,* Wen W. Jiang, John Pratt, Todd Rockway, Kevin Harris, Sudthida Vasavanonda, Rakesh Tripathi, Ron Pithawalla, and Warren M. Kati

Antiviral Research, Infectious Disease Research, Abbott Laboratories, Abbott Park, Illinois 60064-6217

Received March 14, 2006; Revised Manuscript Received August 3, 2006

ABSTRACT: Little is known about the mechanism of HCV polymerase-catalyzed nucleotide incorporation and the individual steps employed by this enzyme during a catalytic cycle. In this paper, we applied various biochemical tools and examined the mechanism of polymerase catalysis. We found that formation of a productive RNA−enzyme complex is the slowest step followed by RNA dissociation and initiation of primer strand synthesis. Various groups have reported several classes of small molecule inhibitors of hepatitis C virus NS5B polymerase; however, the mechanism of inhibition for many of these inhibitors is not clear. We undertook a series of detailed mechanistic studies to characterize the mechanisms of inhibition for these HCV polymerase inhibitors. We found that the diketoacid derivatives competitively bind to the elongation NTP pocket in the active site and inhibit both the initiation and elongation steps of polymerization. While both benzimidazoles and benzothiadiazines are noncompetitive with respect to the active site elongation NTP pocket, benzothiadiazine compounds competitively bind to the initiation pocket in the active site and inhibit only the initiation step of de novo RNA polymerization. The benzimidazoles bind to the thumb allosteric pocket and inhibit the conformational changes during RNA synthesis. We also observed a cross interaction between the thumb allosteric pocket and the initiation pocket using inhibitor−inhibitor cross competition studies. This information will be very important in designing combination therapies using two small molecule drugs to treat hepatitis C virus.

Hepatitis C virus (HCV)[1] is a positive-sense single-stranded RNA virus. The HCV genomic RNA is 9.5 kb in length and consists of a long open reading frame, which is flanked by highly conserved untranslated regions at both the 5′ and 3′ ends. The HCV NS5B gene encodes a RNA-dependent RNA polymerase whose enzymatic activity is critical to the replication of the viral RNA genome. The replication of the plus-strand RNA viral genome consists of two steps: synthesis of the complementary minus-strand RNA with the plus-strand RNA as a template and the subsequent synthesis of the plus-strand RNA genome using the minus-strand RNA as a template. Template-dependent RNA synthesis can be divided into at least four consecutive steps: binding of the enzyme to the template, initiation of RNA synthesis, elongation, and termination. Although it has been demonstrated that HCV NS5B alone can direct RNA replication through a copy-back primer at the 3′ end, de novo initiation of RNA synthesis is likely to be the mode of RNA replication in the infected cells (*1*−*3*). HCV NS5B can accept heterologous viral RNA templates as well as a homogeneous polymeric C template in a primer-independent manner. It can also accept a homogeneous polymeric A template paired with oligo(U) and a homogeneous polymeric C template paired with oligo(G) in a primer-dependent manner (*4*, *5*). In a polymerase reaction, multiple substrates, including a template−primer or a template−initiation nucleotide complex, and an elongation nucleotide are involved. Presumably, reaction at each step follows a sequential order: the polymerase binds to the template−primer first to form a binary complex which then takes up a nucleotide triphosphate to form a ternary complex. The geometry of the priming nucleotide and the elongation nucleotide observed in the catalytic center of HCV NS5B is similar to that observed in the initiation complex of the RNA phage ϕ6 RdRp and suggests that both enzymes might initiate replication by similar mechanisms (*6*−*8*). A high concentration of GTP but not of ATP, CTP, or UTP has been found to stimulate RNA synthesis by up to 2 orders of magnitude. It appears that the high concentration of GTP accelerates a rate-limiting step at the level of initiation of RNA synthesis (*9*).

A significant advance in the understanding of the HCV NS5B polymerase is provided by the crystallographic studies of several truncated forms of the polymerase and its complexes with nucleotides or the RNA template (*10*−*12*). The crystal structure of HCV NS5B reveals a classical "right-hand" shape with the characteristic fingers, palm, and thumb subdomains. The "closed conformation" is formed by a β-hairpin protruding into the active site and a C-terminal region folding from the surface of the thumb toward the active site. These structural elements are likely involved in

* To whom correspondence should be addressed: Dept. R4CQ, Bldg. AP52, Abbott Laboratories, 200 Abbott Park Rd., Abbott Park, IL 60064-6217. Telephone: (847) 937-8626. Fax: (847) 938-2756. E-mail: yaya.liu@abbott.com.

[1] Abbreviations: HCV, hepatitis C virus; RT, reverse transcriptase; RdRp, RNA-dependent RNA polymerase; HEPES, 4-(2-hydroxyethyl)-1-piperazineethanesulfonic acid; PMSF, α-toluenesulfonyl fluoride; SDS, dodecyl sulfate sodium salt; DTT, dithiothreitol; DMSO, dimethyl sulfoxide; IPTG, isopropyl β-D-thiogalactopyranoside.

10.1021/bi060511j CCC: $33.50
Published on Web 09/02/2006

Scheme 1: Mechanism of HCV NS5B Polymerase-Catalyzed RNA Synthesis

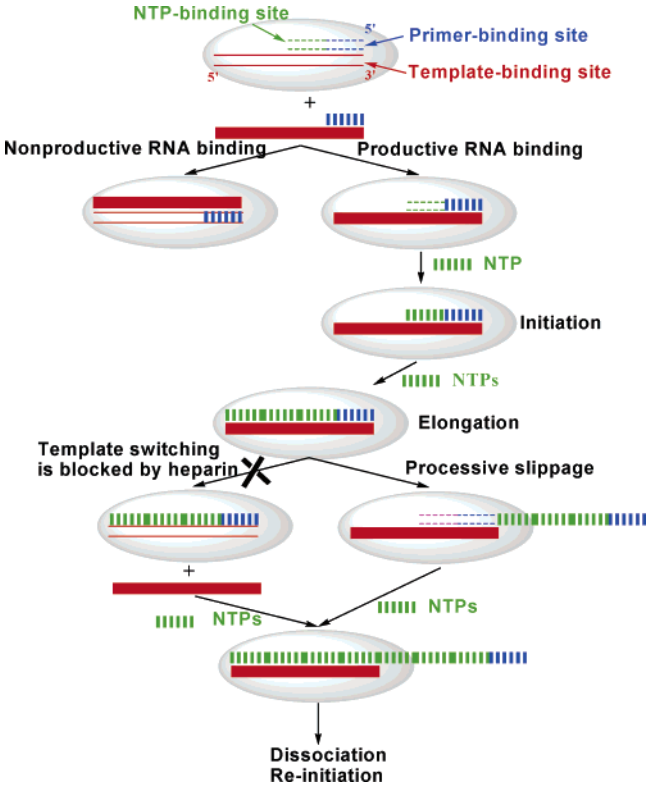

selecting template and de novo initiation. More importantly, they control the protein dynamics during the polymerization reaction. While a significant knowledge of polymerase structure is available, little is known about the mechanism of HCV polymerase-catalyzed nucleotide incorporation and the individual steps employed by this enzyme during a catalytic cycle. This is primarily due to the inability to establish stoichiometric complexes of the enzyme, template−primer, and nucleotide. Processivity, measured under a single processive cycle, is reported to be 700 nucleotides/min on a poly(A)/oligo(U) template and 200 nucleotides/min on a HCV RNA template (*13*, *14*). The HCV polymerase turnover rate is 6000-fold slower than that of Polio Pol^{3D} (*15*) and 10-fold slower than that of HIV RT (*16*). Potential explanations for the discrepancy in k_{cat} and processivity include the following. The active protein concentration is much lower than the total protein concentration. There may be a significant amount of nonproductive RNA binding. Initiation may be rate-limiting. Dissociation may be rate-limiting. Critical viral or cellular cofactors may be missing. In this work, we applied various biochemical tools and examined the polymerase mechanism of catalysis (Scheme 1). We developed a gel-based assay that permitted the separate examination of the initiation and elongation steps. We found that formation of a productive RNA enzyme complex is the slowest step, followed by RNA dissociation and re-initiation.

Various groups have reported several classes of small molecule inhibitors of hepatitis C virus NS5B polymerase. Among the numerous non-nucleoside inhibitors, compounds with either thiophene or phenylalanine scaffolds have been shown to bind to HCV polymerase in the thumb allosteric pocket by X-ray crystal structures (*17*, *18*). A series of compounds based on a benzimidazole scaffold (*19*−*22*) have been reported. Recently, the X-ray crystal structures of benzimidazole scaffold have also been determined and revealed these inhibitors bind to a site on the surface of the thumb domain that is 14 Å from the thumb allosteric pocket that is occupied by compounds of either thiophene or phenylalanine scaffolds (*23*). A series of benzothiadiazine derivatives have also been reported as initiation specific inhibitors (*24*−*27*). The diketoacid derivatives have been reported as product mimics that possibly interact with the catalytic metal ions in the enzyme active site (*28*, *29*). Structures of representative classes of HCV polymerase inhibitors are illustrated in Scheme 2. Despite the extensive biochemical and resistance selection studies for these compounds, it is still not clear whether the mechanism and the site(s) where these three classes of compounds bind on the enzyme are similar. We undertook a series of detailed mechanistic studies to characterize the mechanisms of inhibition for these three classes of polymerase inhibitors. Our studies include kinetic competition of inhibitors with respect to the binding pockets of the initiation nucleotide, elongation nucleotide, and RNA template and kinetic cross competition of inhibitors with respect to the binding pockets of inhibitors with known binding sites. The gel-based assay we developed not only allowed for the separate examination of the initiation and elongation steps but also enabled differentiation of inhibitors targeting the individual chemical steps of the polymerization reaction.

MATERIALS AND METHODS

Materials. Reagents were purchased from the following sources: [^{3}H]UTP, [α-^{33}P]ATP, poly(rA), poly(rC), and nucleotides from Amersham Biosciences, oligonucleotides from MWG Biotech, and T7 Megascript In Vitro Transcription Kit from Ambion. Inhibitors were synthesized by Abbott scientists.

Expression and Purification of HCV NS5B. Recombinant NS5B proteins derived from the NS5B J4 1b strain, the 1a H77 strain, and the patient isolate 1b strain were purified from *Escherichia coli* strain DH5α. The J4 1b strain was obtained from J. Jäger at the University of Leeds (Leeds,

Scheme 2: Chemical Structures of Three Classes of HCV NS5B Polymerase Inhibitors

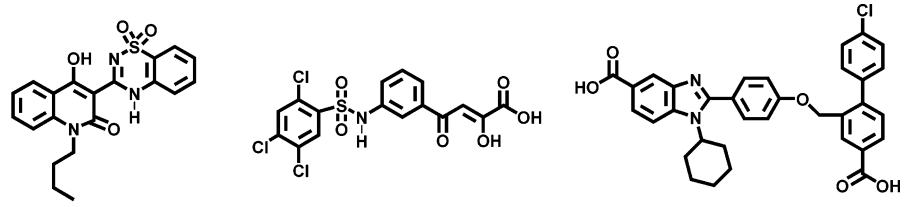

United Kingdom). Patient isolates 1b and 1a H77 were cloned by RT-PCR of HCV RNA isolated from patient serum. The C_{21}-truncated and C_{55}-truncated NS5B proteins contained 570 and 536 native amino acids, respectively, and a tag of six histidines at the N-terminus of the protein for the purpose of affinity chromatographic purification. One liter of TB Broth (Terrific Broth) was inoculated with 10 mL of a starter culture that was at midlog phase (OD_{600} = 0.4−0.6). The inoculated culture was grown at 37 °C until it reached an OD_{600} of 0.6. IPTG was then added to a final concentration of 1 mM, and the culture was grown at room temperature for an additional 4 h. The cell paste isolated from a low-speed spin was resuspended in 20 mL of lysis buffer [50 mM HEPES (pH 8.0), 0.5 M NaCl, 10% glycerol, 2 mM β-mercaptoethanol, and 0.02% sodium azide] that also contained protease inhibitor cocktail tablets from Roche. The cell suspension was passed through a French pressure cell three times at 10 000 psi to lyse the cells. Additional lysis buffer was added to yield a final volume of 40 mL, and then this lysate was centrifuged for 20 min at 10000*g* at 4 °C. The supernatant was dialyzed against 1 L of Ni column buffer (50 mM HEPES, 20 mM imidazole, 0.5 M NaCl, 27.5% glycerol, 2 mM β-mercaptoethanol, 0.2 mM PMSF, and 0.02% sodium azide) at 4 °C for 2 h and then overnight after buffer exchange. The dialyzed supernant was loaded onto a 10 mL Ni column (Talon). The flow-through was collected, and the column was washed with 10 column volumes of Ni column buffer. The bound protein was eluted with Ni column buffer containing 0.35 M imidazole. All polymerase preparations are free of nuclease contamination as assayed from the commercial RNase assay kit.

Preparation of RNA Templates. Large quantities of RNA templates were made from runoff transcription reaction mixtures using the corresponding T7 promoter containing PCR DNA templates and the Ambion T7 Megascript In Vitro Transcription Kit. These RNA templates were further purified using an RNeasy kit. The specific activity of labeled RNA was determined to be 1000 cpm/100 ng of RNA from a standard curve of RNA dose.

Polymerase Assays. The enzymatic activity of HCV polymerase was measured by detecting the incorporation of [^{3}H]UTP into RNA transcripts. The binding of HCV polymerase to RNA was assessed by detecting the bound radiolabeled HCV RNA template. Polymerase (50 nM) was preincubated with 20 nM HCV RNA template containing the 651 nucleotides from the HCV 3′-NTR RNA template, in 50 μL of 20 mM Tris-HCl (pH 7.4), 50 mM NaCl, 1 mM EDTA, 5 mM $MgCl_2$, ATP, CTP, and GTP (40 μM each), 0.61 μM (0.5 μCi) [^{3}H]UTP, and 20 units of RNase inhibitor from Promega. Binding assays were conducted in a similar fashion except that the RNA was labeled with tritium, and the reaction mixture did not contain NTPs. Reaction mixtures were incubated for 2 h at 25 °C in the activity assay or for 1 h at room temperature for the binding assay. Polymerase assays were then stopped with 50 μL of 500 mM EDTA, and then 90 μL of the reaction mixture was transferred onto a DEAE filter plate (Millipore), washed three times with 200 μL of 0.3 M $CHOONH_4$, washed three times with 100 μL of ethanol, and then air-dried for 30 min. For the binding assay, 45 μL of the binding reaction mixture was transferred onto a nitrocellulose filter plate (Millipore) and then washed three times with 50 μL of assay buffer. The amount of incorporated [^{3}H]UTP or bound labeled RNA was measured by scintillation counting on a Wallac 1450 MicroBeta counter after adding 30 μL of Supermix scintillant.

Gel-Based Initiation and Elongation Assays. A 23-mer RNA template (21 nucleotides from the 3′-NTR with additional two Cs added to the 3′ end, 5′-UGGCCUCU-CUGCAGAUCAUGUCC-3′) was employed for the gel-based assay. This shorter RNA substrate allows a better separation of various lengths of RNA products. The assay was carried out in 20 mM Tris, 50 mM NaCl, 1 mM EDTA, 2 mM $MnCl_2$ (pH 7.4), 5 mM DTT, 0.4 unit/μL RNase inhibitor, 2 μM 23-mer RNA template, 1.13 μM J4 Δ21 polymerase, 1 mM GTP, 40 μM ATP, 40 μM CTP, 40 μM UTP, and 0.8 μL of [α-^{33}P]ATP (10 μCi/μL). When the effects of inhibitors on the elongation phase of the reaction which is completed in seconds are examined, a preincubation of inhibitor with the enzyme over 30 min was included before addition of the other nucleotide substrates. The inhibition of the initiation step was examined by the synthesis of a 3-mer RNA product using two of the four nucleotides in the presence of various concentrations of inhibitor for 30 min. The inhibition of the elongation step was examined by assessing the synthesis of equal to and greater than template-sized RNA products in the presence of all four nucleotides with or without inhibitor for 5 min after a half-hour pre-initiation period using cold GTP and ATP in the absence of inhibitor. The reactions were quenched with 2 μL of SDS (50 mM) and 8 μL of sample loading buffer. Samples were denatured at 70 °C for 5 min before being loaded onto a 25% acrylamide−7 M urea−TBE gel. The gel was run at a constant power of 80 W for 2.75 h and then was exposed overnight in a PhosphorImager from Molecular Dynamics. Bands were quantitated using ImageQuant version 5.2 from Molecular Dynamics.

UTP Competition Assay. Reaction mixtures consisted of a total volume of 50 μL in 20 mM Tris (pH 7.4), 50 mM NaCl, 1 mM EDTA, 5 mM $MgCl_2$, 1 mM DTT, 0.1 unit/μL RNase inhibitor, 8 ng/mL HCV RNA 651 nucleotides from the 3′-NTR, 20 μM ATP and CTP, 300 μM GTP, 200 nM 21 NS5B from the 1b J4 strain or 50 nM Δ55 NS5B from a 1b patient isolate, various [^{3}H]UTP and inhibitor concentrations, and 10% DMSO.

GTP Competition Assay. Reaction mixtures consisted of a total volume of 50 μL in 50 mM Tris (pH 8.0), 5 mM $MgCl_2$, 5 mM DTT, 0.1 unit/μL RNase inhibitor, 11 ng/mL poly(C) template, 50 nM Δ55 NS5B from a 1b patient isolate, various [^{3}H]GTP and inhibitor concentrations, and 5% DMSO.

Inhibitor−Inhibitor Competition Assay. Tris-HCl (20 mM, pH 7.4), 50 mM NaCl, 1 mM EDTA, 2 mM $MnCl_2$, 1 mM DTT, 0.1 mg/mL BSA, 0.1 unit/μL RNase inhibitor, 20 μM ATP and CTP, 60 μM GTP, 0.284 μM (0.5 μCi) 5,6-[^{3}H]-UTP, 0.716 μM UTP, 5 nM HCV 2.1 kb RNA, 10% DMSO, 20 nM HCV genotype 1b J4 Δ21 polymerase, and various concentrations of inhibitors at room temperature were used for J4 1b. The same was used for H77 1a except that 80 mM potassium glutamate substituted for NaCl, the GTP concentration was increased to 125 μM, a HCV genotype 1a Δ21 polymerase was used, and the reactions were conducted at 30 °C.

IC_{50} Calculation. The percent inhibition was calculated from the initial rates of the inhibited reactions relative to

the uninhibited control. IC_{50} values were calculated by fitting percent inhibition at six to eight inhibitor concentrations to eq 1 for weak inhibitors. For potent inhibitors, the initial rates were fit to the tight binding equation (eq 2) to obtain K_i^{app}, where $K_i^{app} = K_i(1 + [S]/K_m)$.

$$\text{inhibition percent} = 100[I]/([I] + IC_{50}) \quad (1)$$

$$V = k_{cat}[S]/2(K_m + [S]) \times \sqrt{(K_i^{app} + [I] - [E])^2 + 4K_i^{app}[E]} - (K_i^{app} + [I] - [E]) \quad (2)$$

Determination of K_d and B_{max} for HCV RNA with HCV Polymerase. The radiolabeled HCV RNA bound to HCV polymerase was captured with a nitrocellulose plate and fit to eq 3 to obtain the K_d and B_{max}.

$$\text{bound RNA} = (B_{max} + [L] + K_d) - \sqrt{(B_{max} + [L] + K_d)^2 - 4B_{max}[L]}/2 \quad (3)$$

Determination of K_i and K_i' for the Inhibitor. Initial rates of polymerization reactions were obtained by end point assays. Apparent K_m and V_{max} values at each inhibitor concentration were obtained from nonlinear regression fitting using the Michaelis−Menten equation. K_i and K_i' were obtained from the *X*-axis intercepts of plots of measured K_m/V_{max} and $1/V_{max}$ versus inhibitor concentration, respectively, where K_i represents the binding affinity of the inhibitor for the free enzyme and K_i' reflects the binding affinity of the inhibitor for the enzyme and substrate complexes.

RESULTS

Productive RNA Binding. The HCV NS5B polymerase can bind to many heterogeneous RNA templates; the sequences can be related or unrelated to HCV (*3*). This nonspecific RNA binding is believed to be due to missing viral or cellular factors. It has been shown that HCV NS5B binds to RNA homopolymers with the following order of specificity: poly(U) > poly(G) > poly(A) > poly(C). Interestingly, there is an inverse correlation between RNA binding and polymerase activity that suggests that strong binding interferes with processivity (*30*). Since productive RNA binding is the first step in the polymerase-catalyzed RNA synthesis (Scheme 1), it was important to investigate how much of the polymerase is able to bind to HCV RNA and how much of the total RNA binding is in the productive binding mode. To answer the first question, an experiment in which various amounts of HCV NS5B were titrated against 20 nM radiolabeled HCV RNA was conducted. An apparent K_d of 47.4 nM for HCV polymerase was obtained. At 47.4 nM HCV polymerase, 10 nM HCV RNA was bound to the polymerase, which corresponded to 21% of the total input polymerase (Figure 1A). In a separate experiment in which 50 nM HCV polymerase was titrated with various amounts of radiolabeled HCV RNA, the titration curve indicated a total of 10.8 nM HCV RNA could be bound by HCV polymerase, which also corresponded to 22% of input polymerase (Figure 1B). Therefore, on average, both experiments indicated that ~20% of a 50 nM solution of HCV polymerase is able to bind to HCV RNA productively and nonproductively. The second question is then how much of this 20% complex is in the productive binding mode. To answer the second question, the polymerase activity was followed after it had been preincubated with HCV RNA substrate over different periods of time in the presence of a RNase inhibitor. The polymerase activity was found to increase as the preincubation time with its HCV RNA substrate increased. Indeed, an overall 20-fold increase in the polymerase activity was observed (Figure 1C,D). More importantly, the total RNA binding over the same period of preincubation time as judged from the radiolabeled RNA binding remained constant. This seems to suggest that nonproductive binding of HCV RNA to the HCV polymerase is a predominant process in the beginning but transitions to a more productively bound form over time. It also seems clear that under these in vitro assay conditions, the productive binding is the slowest step and may take days to accomplish.

Template Switching Is Responsible for Longer-Than-Template-Sized RNA Product Synthesis. A gel-based assay was developed to examine the initiation, elongation, and termination or dissociation steps of the HCV polymerase polymerization reaction. Time courses for the formation of a 3-mer RNA product synthesis using a 23-mer RNA template were obtained, in the presence of either two nucleotides (GTP and ATP) or all four nucleotides. Under both conditions, the 3-mer RNA syntheses displayed a biphasic reaction progress curve. The burst phases likely represent the initiation reaction, and the linear phases may represent the re-initiation reaction that is rate-limited by the dissociation of the RNA products. That the initiation phases under the GTP and ATP and four-nucleotide conditions are superimposable suggests the same rate of initiation under these conditions. The fact that the linear parts of the two curves are different probably reflects the fact that the 3-mer RNA is consumed to make longer products under conditions where all four nucleotides are present, whereas the 3-mer RNA accumulates under the GTP and ATP condition (Figure 2). The time courses with varying concentrations of enzyme, template, and NTPs have confirmed the biphasic progress curve (data not shown). The elongation rate was examined by first allowing initiation of 3-mer RNA products to accumulate using cold GTP and ATP only for a half-hour period and then allowing elongation to proceed in the presence of heparin and all four nucleotides (Figure 3, left panel). The time course of 23-mer and >23-mer product formation also displayed a biphasic progress curve as shown in Figure 3E. The burst phase likely represents the elongation of the cold GGA primer synthesized in the half-hour of the ATP and GTP condition. The linear phase may represent the elongation of the re-initiated 3-mer GGA. Similar to what was found before, the elongation reaction reached completion within seconds, and therefore, it was the fastest step in the polymerization reaction. As described previously (*31*), the polymerase aborts frequently by releasing GGA product before the transition to elongation. The transition from initiation to elongation could be rate-limiting for the elongation reaction but not for the total RNA synthesis, which incorporates more steps, including template switching, more elongation, and dissociation. Therefore, the hot 3-mer GGA that accumulated under four-nucleotide conditions was a result of abortive RNA synthesis from the re-initiation event. In the absence of heparin, considerably longer-than-template-sized RNA products were synthesized (Figure 3, right panel).

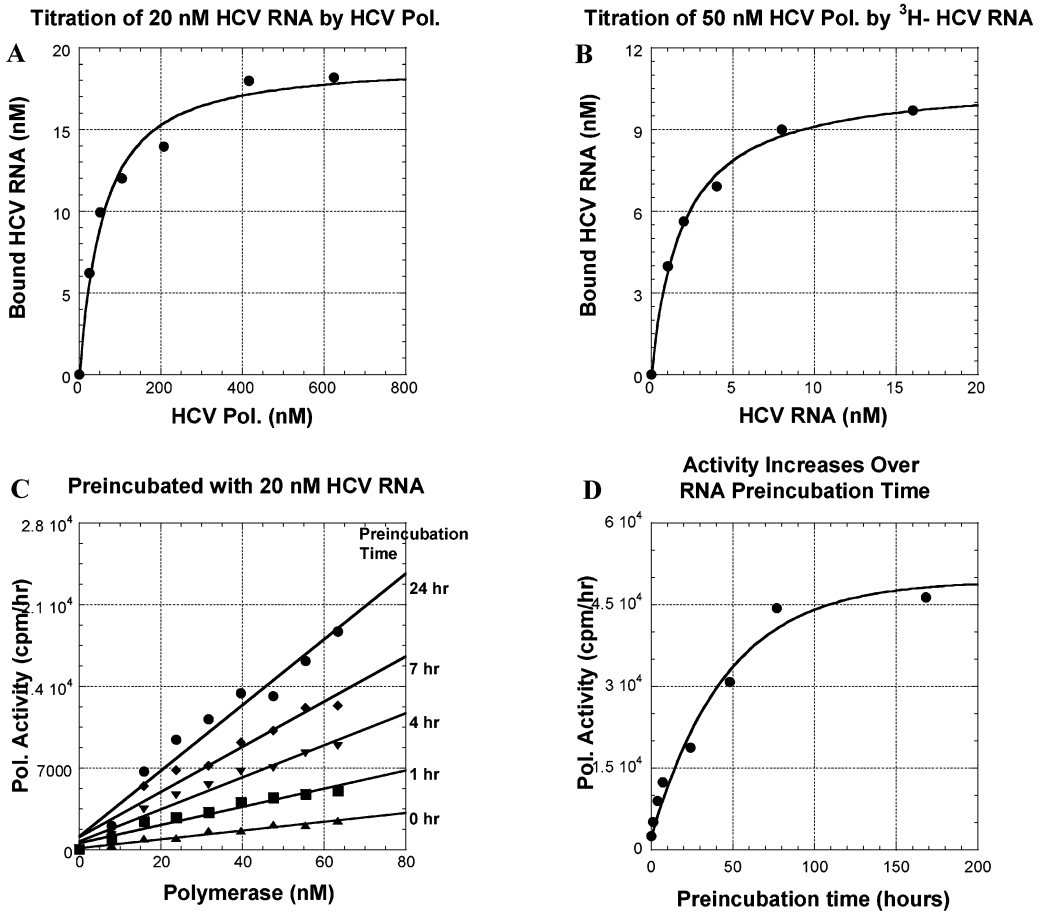

FIGURE 1: Characterization of HCV NS5B polymerase productive RNA binding. (A) Titration curve of 20 nM ^{3}H-labeled HCV RNA by various amounts of HCV NS5B polymerase to provide a K_d value of 47.4 nM. (B) Titration curve of 50 nM HCV NS5B polymerase by various amounts of ^{3}H-labeled HCV RNA to provide a B_{max} (maximum bound) value of 10.8 nM. (C) HCV NS5B polymerase activities assayed after various preincubation times with 20 nM HCV RNA template. (D) Total activity increase of HCV NS5B polymerase upon preincubation with 20 nM HCV RNA template.

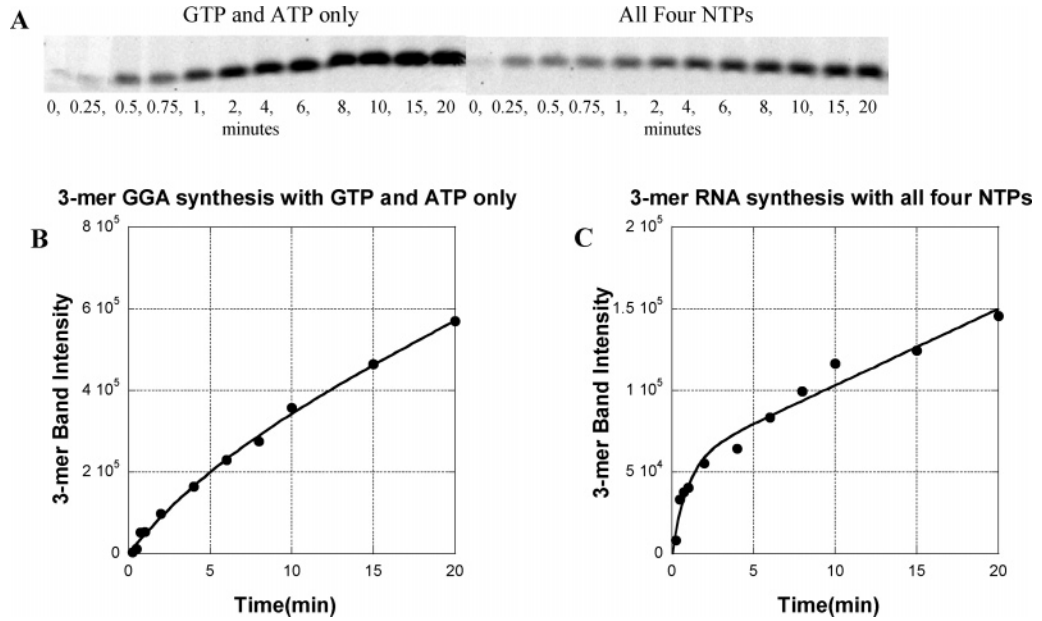

FIGURE 2: Characterization of the initiation step of the polymerization reaction. (A) Gel image of the time courses of 3-mer RNA product GGA syntheses under conditions where GTP and ATP only were present (left side of gel) or when all four nucleotides were present (right side of gel). (B) Graph representation of the time course of 3-mer RNA formation in the presence of GTP and ATP only. (C) Graph representation of the time course of 3-mer RNA formation in the presence of all four NTPs.

These products were mostly formed from a template switching mechanism. Examination of the time course of the template-sized RNA product indicated a loss of 23-mer RNA product over time rather than accumulation of 23-mer

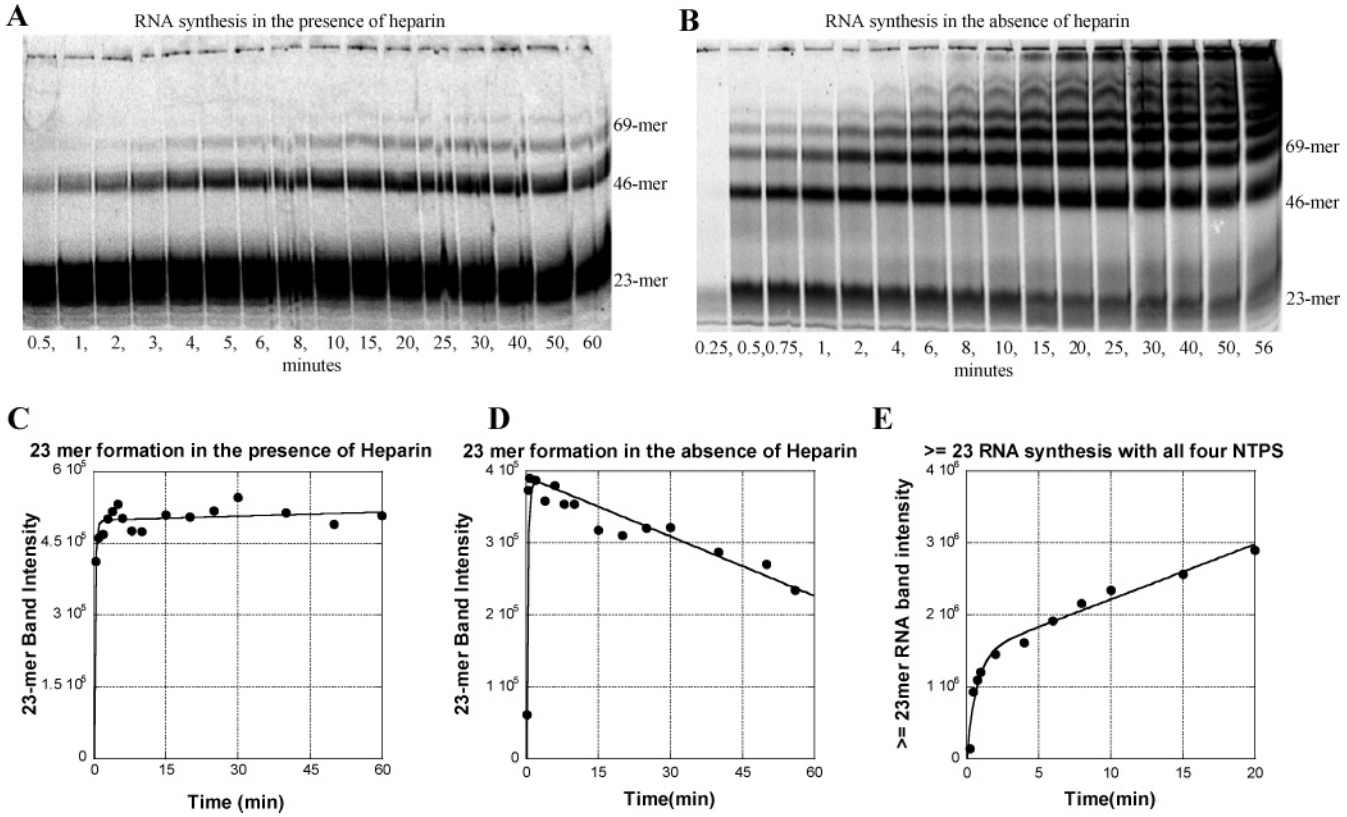

FIGURE 3: Characterization of the elongation step of the polymerization reaction. (A) Gel image of the time course of 23-mer RNA formation in the presence of heparin. (B) Gel image of the time course of 23-mer RNA formation in the absence of heparin. (C) Graph representation of the time course of 23-mer RNA formation in the presence of heparin. (D) Graph representation of the time course of 23-mer RNA formation in the absence of heparin. (E) Graph representation of the time course of species greater than and equal to the template-sized RNA formations in the absence of heparin.

product. The rate of loss of 23-mer was a sum of the rate of 23-mer formation from the re-initiation step and the rate of 23-mer consumption from a template switching step. Therefore, the loss of 23-mer RNA product suggested that the template switching step was faster than re-initiation, which was rate-limited by the RNA product dissociation. On the other hand, one would expect to see an increase in the amount of 23-mer RNA over time if the re-initiation step is faster than template switching.

Differentiation of Initiation and Elongation Inhibitors by a Gel-Based Assay. Most biochemical assays for inhibitor testing involve measurement of the total RNA that was synthesized and do not separate the initiation reaction from the elongation reaction. Therefore, it is unclear whether inhibitors from various classes inhibit the initiation step or the elongation step of polymerization. To address this need, a gel-based assay that allows one to differentiate those two types of inhibitors was developed. It was found that the benzothiadiazine inhibited only the initiation step of the polymerization but not the elongation step, whereas the diketoacid compound inhibited both steps of RNA polymerization (Figure 4A). The 3-mer RNA product synthesized with either benzothiadiazine or diketoacid present gave dose-dependent inhibition curves for the initiation reactions (Figure 4B,C). Interestingly, the intensities of species equal to and longer than the template-sized RNA product in the presence of various concentrations of benzothiadiazine remain unchanged and suggested that the benzothiadiazine did not inhibit the elongation step. On the other hand, the diketoacid not only reduced the total RNA synthesized but also shortened the length of the RNA product and clearly indicated the inhibition of the elongation step (Figure 4D,E). The benzimidazole behaved differently than the diketoacid and the benzothiadiazine. Unlike the benzothiadiazine, it could inhibit RNA synthesis of both 3-mer and longer-than-template-sized RNA. Unlike the diketoacid, it did not slow the elongation step and generated shorter-than-template-sized RNA products (data not shown).

Kinetic Competition with Substrates. The saturation binding curve of elongation UTP nucleotide to the HCV polymerase yielded a K_m of 0.32 μM when assayed with a 651-nucleotide HCV specific RNA template (Figure 5A). Unlike the UTP saturating titration curve, a biphasic response was observed for GTP incorporation, which resulted in two K_m values (Figure 5B,C). The lower value is similar to the K_m values for other nucleotides, which may reflect the binding of nucleotides during elongation. The higher K_m value for GTP may be the result of de novo initiation of RNA synthesis. Both the elongation UTP and initiation GTP substrates were used as competitor ligands for inhibitor characterization studies. We found that the benzothiadiazine was noncompetitive with respect to the elongation NTP with a K_i of 0.14 M but competitive with respect to the initiation GTP (Figure 5D,E). Since the GTP competition assay suffered from a low signal problem and was only feasible with the patient Δ55 C-terminal deletion form of HCV polymerase, we obtained a K_i of 11 μM benzothiadiazine toward the patient Δ55 C-terminal deletion form of HCV polymerase. The difference in binding affinities of benzothiadiazine toward Δ21 and Δ55 C-terminal deletion forms

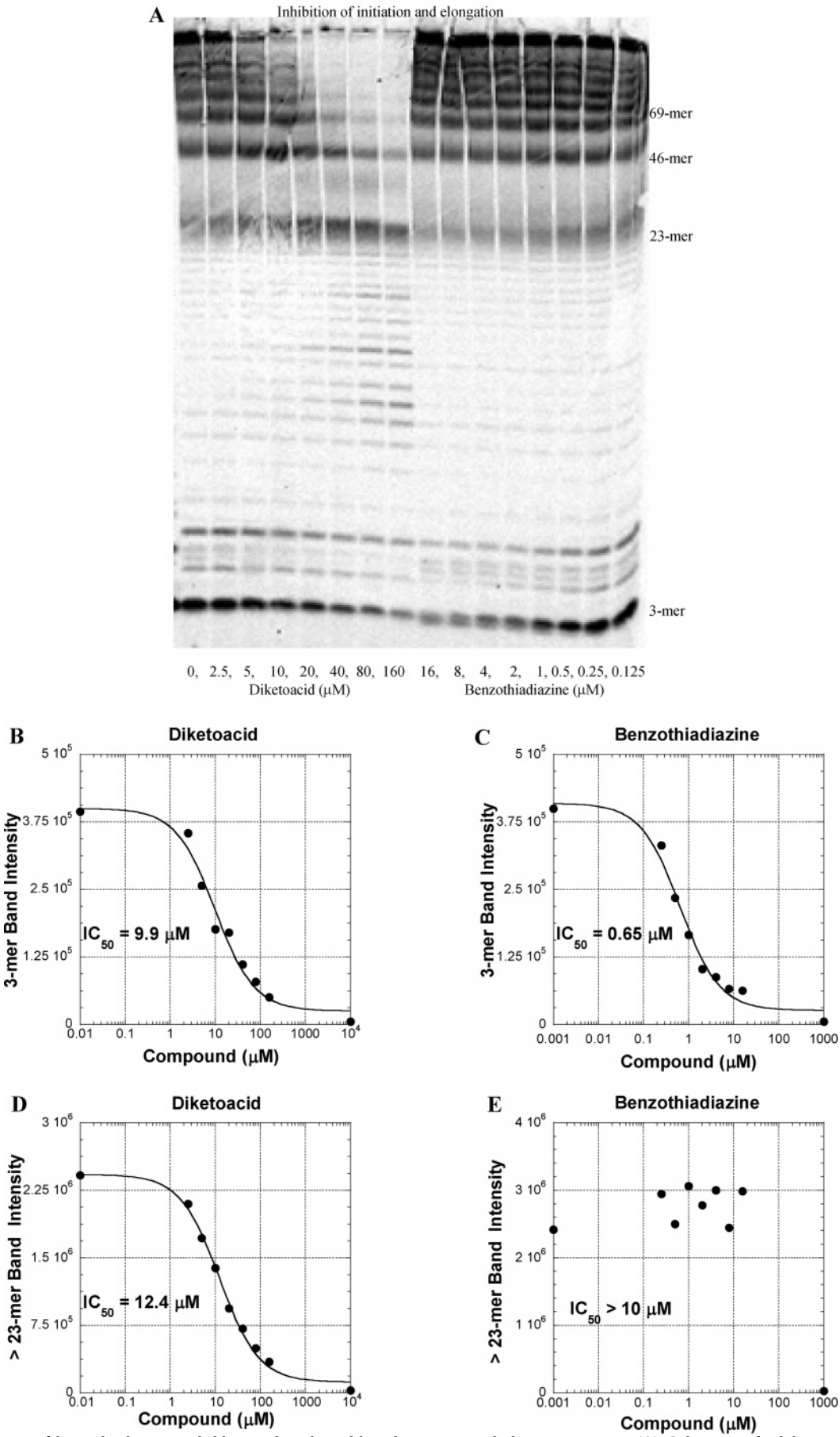

FIGURE 4: Testing of benzothiadiazine and diketoacid in the gel-based initiation and elongation assays. (A) Gel image of inhibition of initiation and elongation steps of the polymerization reaction by diketoacid and benzothiadiazine. Note that in panel A the concentrations of diketoacid and benzothiadiazine increase and decrease, respectively, from left to right. (B) Inhibition curve of the initiation step of the polymerization reaction by diketoacid. (C) Inhibition curve of the initiation step of the polymerization reaction by benzothiadiazine. (D) Inhibition curve of the elongation step of the polymerization reaction by diketoacid. (E) Inhibition curve of the elongation step of the polymerization reaction by benzothiadiazine.

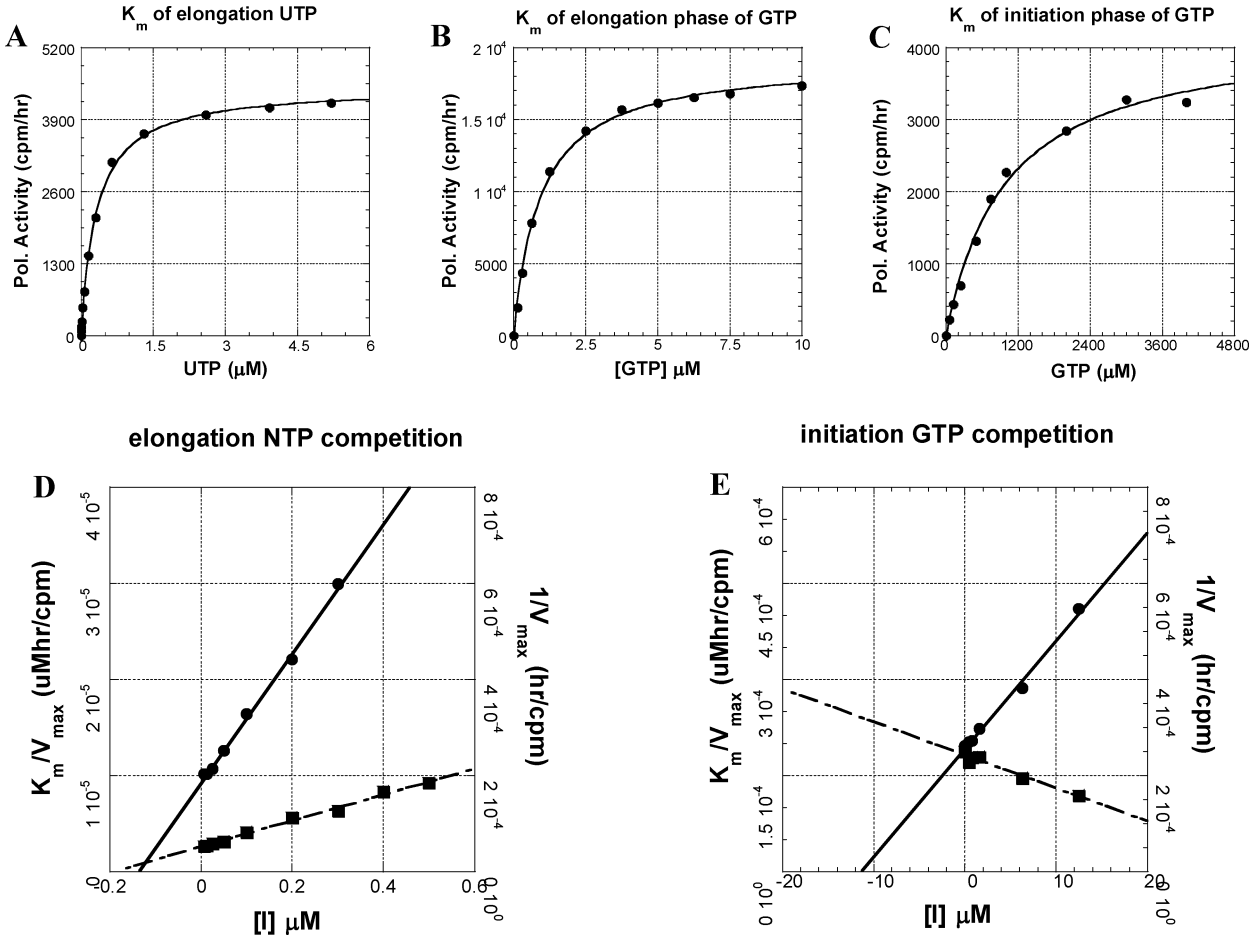

FIGURE 5: Kinetic characterizations of substrates and inhibitors. (A) UTP titration curve that yields a K_m value of 0.32 μM for elongation UTP. (B) GTP titration curve that yields a K_m value of 0.93 M for elongation GTP. (C) GTP titration curve that yields a K_m value of 995 μM for initiation GTP. (D) Benzothiadiazine competition study with respect to elongation NTP using a C-terminal 21-amino acid deletion form of the HCV polymerase. (E) Benzothiadiazine competition study with respect to initiation GTP using a C-terminal 55-amino acid deletion form of the HCV polymerase: (●) K_m/V_{max} values and (■) $1/V_{max}$ values.

of HCV polymerase will be explored in future investigations. The competitiveness of the benzothiadiazine with respect to the initiation GTP agrees very well with the gel-based assay result whereby the benzothiadiazine was found to inhibit only the initiation step of the polymerization reaction. It was also found that the diketoacid was competitive with respect to the elongation NTP but noncompetitive with respect to the initiation GTP (data not shown). This result again agrees with the diketoacid's ability to inhibit both the initiation and the elongation steps of polymerization, presumably by occupying the elongation NTP site. Interestingly, we found that the benzimidazole compound was noncompetitive with respect to both the elongation NTP and the initiation GTP (data not shown). To determine if the benzimidazole compound inhibited the polymerase activity by disrupting the binding of RNA to the polymerase, we examined the benzimidazole's properties with regard to the inhibition of RNA binding and the inhibition of RNA synthesis. The assay for examining the inhibition of binding of RNA to the HCV polymerase was conducted at the exact RNA template and HCV polymerase concentrations as they were in the polymerase activity assay except that no NTPs were added and a radiolabeled RNA template was used. We found that the benzimidazole inhibited polymerase activity with an IC_{50} of 0.12 μM but did not appear to interfere with RNA binding (IC_{50} > 5 μM). Therefore, the benzimidazole is not likely

Table 1: Comparison of Kinetic Constants of Three Classes of Polymerase Inhibitors with Δ21 and Δ55 Forms of HCV NS5B Polymerases

class of compound	K_i with Δ21 polymerase (μM)	K_i with Δ55 polymerase (μM)	K_i difference (Δ55/Δ21)
benzothiadiazine	0.15	5.5	37-fold
diketoacid	0.33	0.42	1.3-fold
benzimidazole	0.12	0.02	0.17-fold

inhibiting HCV polymerase by binding to the RNA template-binding site. Neither the benzothiadiazine nor the diketoacid was shown to inhibit the HCV polymerase by binding to the RNA−template binding site (data not shown).

Inhibitors Display Different Binding Affinities toward C-Terminally Truncated Forms of HCV Polymerase. These three classes of inhibitors were evaluated against forms of 1b HCV polymerase of both amino acids 1−570 and 1−536 isolated from a patient strain (Table 1). Interestingly, the benzothiadiazine displayed a much-reduced binding affinity toward the Δ55 C-terminal deletion form of HCV polymerase relative to the Δ21 C-terminal deletion form of HCV polymerase as previously observed (*27*). Since the benzothiadiazine binds to the initiation nucleotide pocket and this pocket is at least partially formed from the C-terminal residues looping back toward the active site (*10*−*12*), it seems that the initiation pocket is less well defined in the

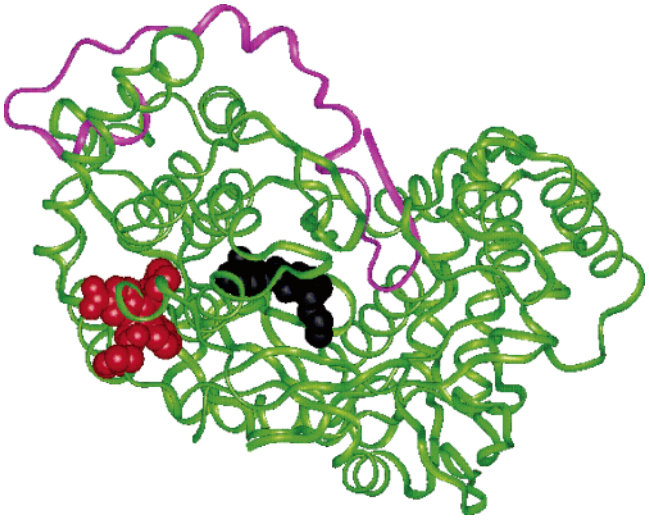

FIGURE 6: Ribbon diagram of the backbone of HCV polymerase (green) from protein X-ray crystallographic studies (PDB entry 1C2P). C-Terminal residues 530−564 are colored pink. The benzimidazole ligand (from PDB entry 2BRK) is colored red. An energy-minimized model of the thiadiazine ligand is colored black and was manually docked to be in surface contact with the known resistance mutation, Met414.

Δ55 C-terminal deletion form of HCV polymerase than it is in the Δ21 C-terminal deletion form of HCV polymerase. Resistance studies also revealed the M414 residue confers a high resistance to the thiadiazine compound (*32*). On the other hand, the benzimidazole compound was 5-fold more potent against the Δ55 C-terminal deletion form of HCV polymerase relative to the Δ21 C-terminal deletion form of HCV polymerase. The diketoacid that binds to the elongation NTP pocket was equally active against both forms of the polymerase. A ribbon diagram of the backbone of HCV polymerase (green) from protein X-ray crystallographic studies is shown in Figure 6 (PDB entry 1C2P) with C-terminal residues 530−564 colored pink and the benzimidazole ligand (from PDB entry 2BRK) colored red. An energy-minimized model of the thiadiazine ligand is colored black and was manually docked to be in surface contact with the known resistance mutation, Met414.

Kinetic Competition with Inhibitors. Inhibitors of known binding sites could be used as probes to study inhibitors of unknown binding sites with regard to whether their binding sites are overlapping or completely distinct from each other by using a cross competition assay as described by Yonetani and Theorell (*33*). Three outcomes are possible. A mutually exclusive competitive inhibition pattern will emerge if two inhibitors bind to the same site on the enzyme, thereby excluding each other from the binding site. A mutually exclusive competition inhibition pattern will also emerge if one inhibitor binds to a site that alters the conformation of the enzyme, thereby leading to reduced affinity for the second inhibitor binding at the second site. A synergistic inhibition scenario represents a second possible outcome whereby the binding of one inhibitor results in improved binding affinity for the second inhibitor. The third possible outcome is the additive inhibition scenario whereby both inhibitors bind to the enzyme independently and the binding of one inhibitor has no effect on the binding affinity of the second. Yonetani−Theorell cross competition studies were conducted using the benzothiadiazine and various classes of polymerase inhibitors. A mutually exclusive pattern of inhibition was observed when two benzothiadiazines were combined (data not shown) and an additive pattern of inhibition when a benzothiadiazine and a diketoacid were combined (Figure 7A). Surprisingly, a mutually exclusive pattern of inhibition was also observed when a benzothiadiazine and a benzimidazole were combined (Figure 7B).

DISCUSSION

Although homogeneous active preparations of HCV polymerase have been available for several years (*34*−*37*), very little is known about the mechanism of RNA template binding, nucleotide initiation, and elongation catalyzed by this enzyme during a catalytic cycle. This is primarily due to the inability to establish stoichiometric complexes of the enzyme, template−primer, and nucleotide. It was reported that only less than 1% of the HCV NS5B polymerase is catalytically competent (*14*). To account for their finding, the authors speculated about several reasons such as (a) the incorrect folding of the majority of the protein, (b) the possible presence of a tightly bound inhibitor that arises during either expression or purification, (c) significant nonproductive binding to the RNA template, and (d) missing viral or cellular cofactors. The initial goal of this study was to systematically examine the HCV polymerase-catalyzed

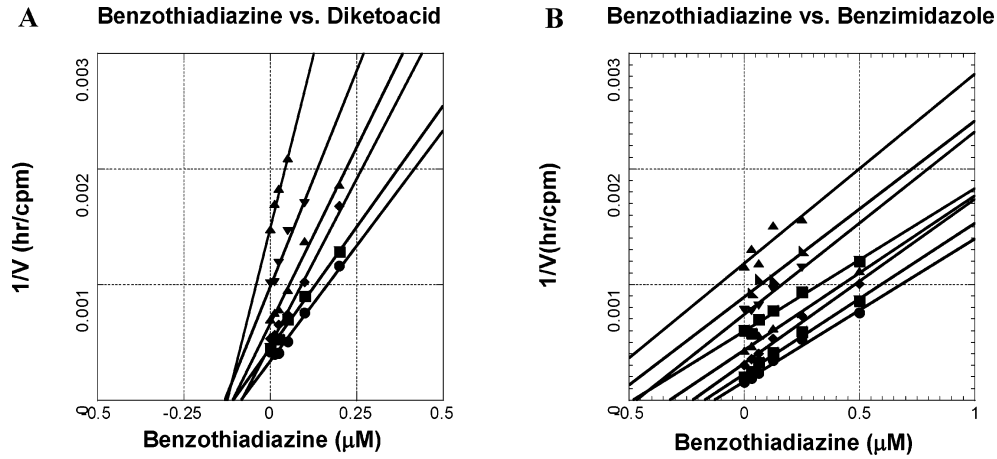

FIGURE 7: Yonetani−Theorell kinetic competition study of two inhibitors. (A) Combination of various concentrations of benzothiadiazine with various concentrations of diketoacid. (B) Combination of various concentrations of benzothiadiazine with various concentrations of benzimidazole.

Scheme 3: Chemical Steps of HCV Polymerase-Catalyzed RNA Synthesis in the Absence of Heparin

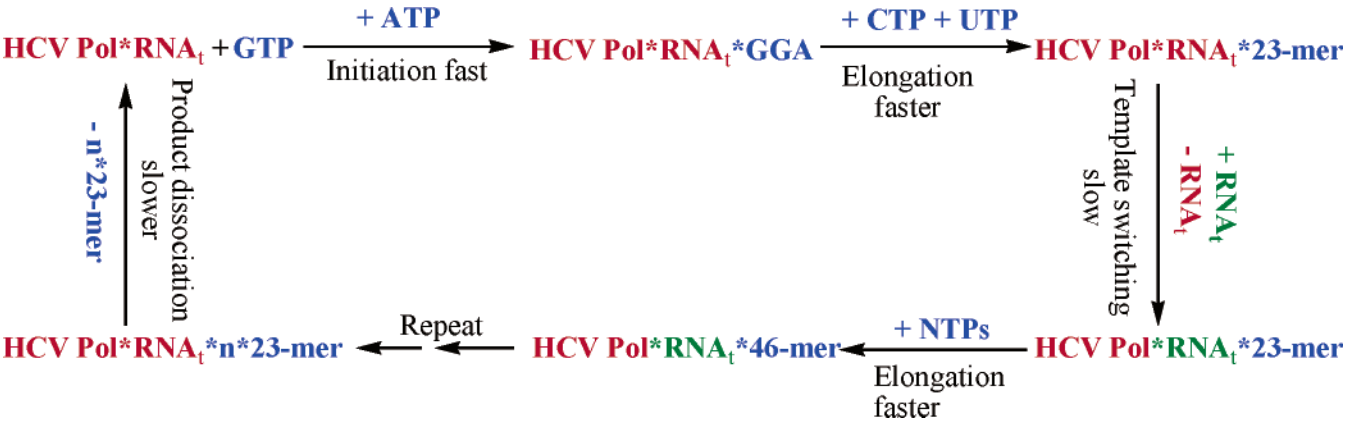

polymerization steps individually and to answer those questions. The investigations started from the very first step, RNA template binding, and addressed questions such as what percentage of the HCV polymerase is able to bind to the template RNA, how much of the binding is in the productive RNA binding mode, and does the productive RNA binding increase during the preincubation with the enzyme. Unlike the previously reported result that less than 1% of purified HCV polymerase is catalytically competent (*14*), we found that 20% of the HCV polymerase is able to bind to HCV RNA but that the level of productive RNA binding starts from 1% and increases over time, eventually achieving a 20-fold increase in the rate of the polymerase-catalyzed RNA synthesis. The differences in the enzyme preparations and the RNA template might also be attributed to the difference in the percent of active polymerase. We found the formation of a productive RNA template polymerase complex appears to be a very slow step in the in vitro enzyme assay as previously observed (*14*, *27*). This is perhaps due to missing viral or cellular factors that might stimulate formation of a productive polymerase−RNA complex. Recent studies have suggested that the cellular peptidyl prolyl cis−trans isomerase cyclophilin B might perform this function within cells. Cyclophilin B has been demonstrated to be critical for the efficient replication of the HCV genome within cells and directly stimulates the ability of HCV polymerase to bind RNA (*38*).

The initiation reaction was then examined by monitoring 3-mer GGA RNA product formation using a 23-mer RNA template under conditions where only two nucleotides were present or conditions where all four nucleotides were present. A biphasic product formation under both conditions was found, with superimposable initial burst phases in the initial 60 s, and much slower phases later in the reaction time course. The initial burst phase represented the initiation reaction, while the latter slower phase represented the re-initiation reaction that is presumably rate limited by the RNA product dissociation. The elongation reaction was examined in the presence and absence of heparin. In the presence of heparin, the elongation reached completion within seconds. Therefore, consistent with the literature information (*13*, *14*), the HCV polymerase is quite processive. A few longer-than-template-sized RNA products were synthesized in the presence of heparin in Figure 3A due to the processive slippage mechanism (*30*). In the absence of heparin, the majority of the RNA synthesized was longer than the template size and was a result of the template switching mechanism (*30*). The decrease in the level of template-sized RNA over time would suggest that the template switching step is faster than the re-initiation given the fact that elongation is much faster than these two steps. In summary, these studies demonstrated that formation of a productive RNA complex is the slowest step during in vitro HCV polymerase-catalyzed RNA synthesis, followed by the re-initiation step, which is rate-limited by the dissociation of the RNA product. A template switching step is responsible for longer-than-template-sized RNA product synthesis. Most of the HCV polymerase gel-based biochemical assays are based on signals from the total RNA synthesis (*39*−*41*). These assays are a combination of both initiation reaction and elongation reactions. While many classes of polymerase inhibitors have been disclosed in the literature, few have been shown to inhibit specific steps of polymerization. Therefore, it is important to understand which steps of the polymerization reaction are blocked by specific inhibitor classes. The gel-based assay allowed the differentiation of initiation specific inhibitors from the elongation specific inhibitors. While several lines of evidence have been shown to suggest that the benzothiadiazine is an initiation inhibitor (*24*, *27*), our data provide direct evidence that the benzothiadiazine is an initiation specific inhibitor and does not inhibit the elongation step once the initiation step starts. It is the first time that we can demonstrate that the diketoacid not only inhibited the initiation step but also inhibited the elongation step. The benzimidazole behaved in a manner different from that of the diketoacid and the benzothiadiazine and inhibited conformational changes during RNA synthesis as suggested from the X-ray crystal structure reported previously (*19*, *23*).

GTP was observed to bind to HCV polymerase with high affinity as well as low affinity. The K_m of high-binding affinity GTP is 0.94 μM, which is similar to the K_m of 0.32 μM for UTP. Since the same elongation NTP pocket is used during the elongation phase of RNA synthesis, the high binding affinity of GTP likely represents the binding affinity of GTP in the elongation NTP pocket. Interestingly, at a higher GTP concentration, a significant amount of stimulation of RNA synthesis was observed and yielded a low binding affinity for GTP with a K_m of 1 mM. This stimulation is not seen with any other nucleotides. There have also been several other studies reported in the literature about the GTP as the initiation nucleotide of RNA synthesis by HCV NS5B polymerase and swine fever virus NS5B polymerase (*9*), BVDV polymerase, and GB virus B (*42*−*44*). It has been

shown that the stimulation of RNA synthesis by polymerases is not due to an enhancement of RNA binding or an increase of the elongation rate at higher GTP concentrations (*9*). Instead, the low binding affinity of GTP likely represents the low-affinity binding of GTP to the initiation nucleotide pocket. It is also interesting to note that the low-affinity surface GTP binding site, while specific and with a binding affinity approximately similar to our observed initiation GTP nucleotide binding affinity, appears to have no consequence on polymerase activity (*8, 19*). When both high- and low-affinity nucleotide substrate conditions are used as probes for inhibitor binding, we found that the diketoacid derivatives competitively bind to the high-affinity elongation NTP pocket in the active site and that while both benzimidazole compounds and benzothiadiazine compounds bind noncompetitively to the high-affinity elongation NTP pocket, the benzothiadiazine compounds competitively bind to the low-affinity initiation GTP pocket in the active site. These results are consistent with the gel-based assay data which show that the benzothiadiazine is an initiation specific inhibitor and that the diketoacid can inhibit both the initiation and elongation steps with equal effectiveness.

The difference in affinities for binding of these three classes of inhibitors to the C-terminal 21-amino acid deletion form and the C-terminal 55-amino acid deletion form of the polymerase is significant. The benzothiadiazine was a much weaker inhibitor toward the C-terminal 55-amino acid deletion form of the HCV polymerase. This is likely due to an incompletely formed initiation pocket in this form of the enzyme due to the absence of the C-terminal tail, which normally protrudes into the active site (*10*−*12*, *27*) (Figure 6). The benzimidazole, on the other hand, exhibited slightly more potent binding toward the C-terminal 55-amino acid deletion form of the HCV polymerase. This surprising result can now be rationalized on the basis of the recently determined X-ray crystal structure of a benzimidazole compound bound to HCV polymerase (*23*). The benzimidazole was shown to bind to a site on the surface of the thumb domain. The thumb pocket is formed from C-terminal residues 371−528 and is affected by the C-terminal truncations. Indeed, the tighter binding for the benzimidazole compound to the C-terminally truncated form suggests that this is the case. In addition, the inhibitor cross competition study of benzothiadiazine and benzimidazole indicated a mutually exclusive pattern suggesting a cross interaction between the thumb allosteric pocket and the initiation pocket. This cross interaction between the thumb allosteric pocket and the initiation pocket is supported by the structure feature of the C-terminal region folding from the surface of the thumb toward the active site and controlling the protein dynamics during the polymerization reaction (*45*). We know from both X-ray crystal structure and resistant selection studies that the benzimidazole binds to the thumb allosteric pocket and the benzothiadiazine binds to the initiation platform. Although further work will be required to establish the exact mechanism for the benzimidazole carboxylate, these studies provide the first direct evidence for an allosteric effect between the benzimidazole carboxylate binding site and the initiation platform.

The high HCV copy number, the significant diversity of the quasi-species that are present in HCV-infected patients, and the high potential for the development of resistance suggest that multiple drugs will likely be required to effectively treat this disease. Therefore, it becomes important to understand the mechanisms of inhibition for each drug individually as well as to identify any adverse or synergistic effects that certain drug combinations might exhibit. For example, the additive inhibitory effects of combining a benzothiadaizine and a diketoacid would likely predict a favorable clinical outcome in treating HCV disease, whereas the mutually exclusive effect of combining a benzothiadiazine and a benzimidazole may be less desirable. These biochemical kinetic studies will be useful for characterizing new HCV polymerase inhibitors and for choosing the best inhibitor combinations for further drug discovery efforts.

ACKNOWLEDGMENT

We thank Rohinton Edalji, Wenying Qin, and Sally Dorwin for purifying the polymerases, Chih-Ming Chen for his gel separation condition, and Tim Middleton for providing the 23-mer RNA template. We are grateful to Kent Stewart for his picture representation of C-terminal residues and binding sites of the HCV polymerase structure.

REFERENCES

1. Behrens, S. E., Tomei, L., and De-Francesco, R. (1996) Identification and properties of the RNA-dependent RNA polymerase of hepatitis C virus, *EMBO J. 15* (1), 12−22.
2. Lohmann, V., Körner, F., Herian, U., and Bartenschlager, R. (1997) Biochemical properties of hepatitis C virus NS5B RNA-dependent RNA polymerase and identification of amino acid sequence motifs essential for enzymatic activity, *J. Virol. 71* (11), 8416−8428.
3. Oh, J. W., Ito, T., and Lai, M. M. (1999) A recombinant hepatitis C virus RNA-dependent RNA polymerase capable of copying the full-length viral RNA, *J. Virol. 73* (9), 7694−7702.
4. Lohmann, V., Roos, A., Körner, F., Koch, J. O., and Bartenschlager, R. (1998) Biochemical and kinetic analyses of NS5B RNA-dependent RNA polymerase of the hepatitis C virus, *Virology 249* (1), 108−118.
5. Ferrari, E., Wright-Minogue, J., Fang, J. W., Baroudy, B. M., Lau, J. Y., and Hong, Z. (1999) Characterization of soluble hepatitis C virus RNA-dependent RNA polymerase expressed in *Escherichia coli*, *J. Virol. 73* (2), 1649−1654.
6. Butcher, S. J., Grimes, J. M., Makeyev, E. V., Bamford, D. H., and Stuart, D. I. (2001) A mechanism for initiating RNA-dependent RNA polymerization, *Nature 410* (6825), 235−240.
7. Laurila, M. R. L., Makeyev, E. V., and Bamford, D. H. (2002) Bacteriophage ϕ6 RNA-dependent RNA polymerase: Molecular details of initiating nucleic acid synthesis without primer, *J. Biol. Chem. 277* (19), 17117−17124.
8. Bressanelli, S., Tomei, L., Rey, F. A., and De-Francesco, R. (2002) Structural analysis of the hepatitis C virus RNA polymerase in complex with ribonucleotides, *J. Virol. 76* (7), 3482−3492.
9. Lohmann, V., Overton, H., and Bartenschlager, R. (1999) Selective stimulation of hepatitis C virus and pestivirus NS5B RNA polymerase activity by GTP, *J. Biol. Chem. 274* (16), 10807−10815.
10. Lesburg, C. A., Cable, M. B., Ferrari, E., Hong, Z., Mannarino, A. F., and Weber, P. C. (1999) Crystal structure of the RNA-dependent RNA polymerase from hepatitis C virus reveals a fully encircled active site, *Nat. Struct. Biol. 6* (10), 937−943.
11. O'Farrell, D., Trowbridge, R., Rowlands, D., and Jäger, J. (2003) Substrate complex of hepatitis C virus RNA polymerase (HC-J4): Structural evidence for nucleotide import and *de-novo* initiation, *J. Mol. Biol. 326* (4), 1025−1035.
12. Bressanelli, S., Tomei, L., Roussel, A., Incitti, I., Vitale, R. L., Mathieu, M., De-Francesco, R., and Rey, F. A. (1999) Crystal structure of the RNA-dependent RNA polymerase of hepatitis C virus, *Proc. Natl. Acad. Sci. U.S.A. 96* (23), 13034−13039.
13. Tomei, L., Vitale, R. L., Incitti, I., Serafini, S., Altamura, S., Vitelli, A., and De-Francesco, R. (2000) Biochemical characterization of a hepatitis C virus RNA-dependent RNA polymerase mutant lacking the C-terminal hydrophobic sequence, *J. Gen. Virol. 81* (Part 3), 759−767.
14. Carroll, S. S., Sardana, V., Yang, Z., Jacobs, A. R., Mizenko, C., Hall, D., Hill, L., Zugay-Murphy, J., and Kuo, L. C. (2000) Only

a small fraction of purified hepatitis C RNA-dependent RNA polymerase is catalytically competent: Implications for viral replication and in vitro assays, *Biochemistry 39* (28), 8243−8249.
15. Van Dyke, T. A., Rickles, R. J., and Flanegan, J. B. (1982) Genome-length copies of poliovirion RNA are synthesized in vitro by the poliovirus RNA-dependent RNA polymerase, *J. Biol. Chem. 257*, 4610−4617.
16. Reardon, J. E. (1992) Human immunodeficiency virus reverse transcriptase: Steady-state and pre-steady-state kinetics of nucleotide incorporation, *Biochemistry 31*, 4473−4479.
17. Wang, M., Ng, K. K. S., Cherney, M. M., Chan, L., Yannopoulos, C. G., Bedard, J., Morin, N., Nguyen, B. N., Alaoui, I. M. H., Bethell, R. C., and James, M. N. G. (2003) Non-nucleoside analogue inhibitors bind to an allosteric site on HCV NS5B polymerase. Crystal structures and mechanism of inhibition, *J. Biol. Chem. 278* (11), 9489−9495.
18. Love, R. A., Parge, H. E., Yu, X., Hickey, M. J., Diehl, W., Gao, J., Wriggers, H., Ekker, A., Wang, L., Thomson, J. A., Dragovich, P. S., and Fuhrman, S. A. (2003) Crystallographic identification of a noncompetitive inhibitor binding site on the hepatitis C virus NS5B RNA polymerase enzyme, *J. Virol. 77* (13), 7575−7581.
19. Tomei, L., Altamura, S., Bartholomew, L., Biroccio, A., Ceccacci, A., Pacini, L., Narjes, F., Gennari, N., Bisbocci, M., Incitti, I., Orsatti, L., Harper, S., Stansfield, I., Rowley, M., De-Francesco, R., and Migliaccio, G. (2003) Mechanism of action and antiviral activity of benzimidazole-based allosteric inhibitors of the hepatitis C virus RNA-dependent RNA polymerase, *J. Virol. 77* (24), 13225−13231.
20. McKercher, G., Beaulieu, P. L., Lamarre, D., LaPlante, S., Lefebvre, S., Pellerin, C., Thauvette, L., and Kukolj, G. (2004) Specific inhibitors of HCV polymerase identified using an NS5B with lower affinity for template/primer substrate, *Nucleic Acids Res. 32* (2), 422−431.
21. Beaulieu, P. L., Bös, M., Bousquet, Y., DeRoy, P., Fazal, G., Gauthier, J., Gillard, J., Goulet, S., McKercher, G., Poupart, M., Valois, S., and Kukolj, G. (2004) Non-nucleoside inhibitors of the hepatitis C virus NS5B polymerase: Discovery of benzimidazole 5-carboxylic amide derivatives with low-nanomolar potency, *Bioorg. Med. Chem. Lett. 14* (4), 967−971.
22. Beaulieu, P. L., Bös, M., Bousquet, Y., Fazal, G., Gauthier, J., Gillard, J., Goulet, S., LaPlante, S., Poupart, M., Lefebvre, S., McKercher, G., Pellerin, C., Austel, V., and Kukolj, G. (2004) Non-nucleoside inhibitors of the hepatitis C virus NS5B polymerase: Discovery and preliminary SAR of benzimidazole derivatives, *Bioorg. Med. Chem. Lett. 14* (1), 119−124.
23. Di-Marco, S., Volpari, C., Tomei, L., Altamura, S., Harper, S., Narjes, F., Koch, U., Rowley, M., De-Francesco, R., Migliaccio, G., and Carfí, A. (2005) Interdomain Communication in Hepatitis C Virus Polymerase Abolished by Small Molecule Inhibitors Bound to a Novel Allosteric Site, *J. Biol. Chem. 280* (33), 29765−29770.
24. Gu, B., Johnston, V. K., Gutshall, L. L., Nguyen, T. T., Gontarek, R. R., Darcy, M. G., Tedesco, R., Dhanak, D., Duffy, K. J., Kao, C. C., and Sarisky, R. T. (2003) Arresting initiation of hepatitis C virus RNA synthesis using heterocyclic derivatives, *J. Biol. Chem. 278* (19), 16602−16607.
25. Dhanak, D., Duffy, K. J., Johnston, V. K., Lin, G. J., Darcy, M., Shaw, A. N., Gu, B., Silverman, C., Gates, A. T., Nonnemacher, M. R., Earnshaw, D. L., Casper, D. J., Kaura, A., Baker, A., Greenwood, C., Gutshall, L. L., Maley, D., DelVecchio, A., Macarron, R., Hofmann, G. A., Alnoah, Z., Cheng, H. Y., Chan, G., Khandekar, S., Keenan, R. M., and Sarisky, R. T. (2002) Identification and biological characterization of heterocyclic inhibitors of the hepatitis C virus RNA-dependent RNA polymerase, *J. Biol. Chem. 277* (41), 38322−38327.
26. Nguyen, T. T., Gates, A. T., Gutshall, L. L., Johnston, V. K., Gu, B., Duffy, K. J., and Sarisky, R. T. (2003) Resistance profile of a hepatitis C virus RNA-dependent RNA polymerase benzothiadiazine inhibitor, *Antimicrob. Agents Chemother. 47* (11), 3525−3530.
27. Tomei, L., Altamura, S., Bartholomew, L., Bisbocci, M., Bailey, C., Bosserman, M., Cellucci, A., Forte, E., Incitti, I., Orsatti, L., Koch, U., De-Francesco, R., Olsen, D. B., Carroll, S. S., and Migliaccio, G. (2004) Characterization of the inhibition of hepatitis C virus RNA replication by nonnucleosides, *J. Virol. 78* (2), 938−946.
28. Summa, V., Petrocchi, A., Pace, P., Matassa, V. G., De- Francesco, R., Altamura, S., Tomei, L., Koch, U., and Neuner, P. (2004) Discovery of α,γ-diketo acids as potent selective and reversible inhibitors of hepatitis C virus NS5b RNA-dependent RNA polymerase, *J. Med. Chem. 47* (1), 14−17.
29. Summa, V., Petrocchi, A., Matassa, V. G., Taliani, M., Laufer, R., De-Francesco, R., Altamura, S., and Pace, P. (2004) HCV NS5b RNA-Dependent RNA Polymerase Inhibitors: From α,γ-Diketoacids to 4,5-Dihydroxypyrimidine- or 3-Methyl-5-hydroxypyrimidinonecarboxylic Acids. Design and Synthesis, *J. Med. Chem. 47* (22), 5336−5339.
30. Arnold, J. J., and Cameron, C. E. (1999) Poliovirus RNA-dependent RNA Polymerase ($3D^{pol}$) Is Sufficient for Template Switching *in Vitro*, *J. Biol. Chem. 274* (5), 2706−2716.
31. Shim, J. H., Larson, G., Wu, J. Z., and Hong, Z. (2002) Selection of 3′-template bases and initiation nucleotides by hepatitis C virus NS5B RNA-dependent RNA polymerase, *J. Virol. 76* (14), 7030−7039.
32. Mo, H., Lu, L., Pilot-Matias, T., Pithawalla, R., Mondal, R., Masse, S., Dekhtyar, T., Ng, T., Koev, G., Stoll, V., Stewart, K. D., Pratt, J., Donner, P., Rockway, T., Maring, C., and Molla, A. (2005) Mutations Conferring Resistance to a Hepatitis C Virus (HCV) RNA-Dependent RNA Polymerase Inhibitor Alone or in Combination with an HCV Serine Protease Inhibitor In Vitro, *Antimicrob. Agents Chemother. 49* (10), 4305−4314.
33. Yonetani, T., and Theorell, H. (1964) Studies on liver alcohol dehydrogenase complexes. III. Multiple inhibition kinetics in the presence of two competitive inhibitors, *Arch. Biochem. Biophys. 106*, 243−251.
34. Yuan, Z. H., Kumar, U., Thomas, H. C., Wen, Y. M., and Monjardino, J. (1997) Expression, purification, and partial characterization of HCV RNA polymerase, *Biochem. Biophys. Res. Commun. 232* (1), 231−235.
35. Al, R. H., Xie, Y., Wang, Y., and Hagedorn, C. H. (1998) Expression of recombinant hepatitis C virus non-structural protein 5B in *Escherichia coli*, *Virus Res. 53* (2), 141−149.
36. Yamashita, T., Kaneko, S., Shirota, Y., Qin, W., Nomura, T., Kobayashi, K., and Murakami, S. (1998) RNA-dependent RNA polymerase activity of the soluble recombinant hepatitis C virus NS5B protein truncated at the C-terminal region, *J. Biol. Chem. 273* (25), 15479−15486.
37. Ishii, K., Tanaka, Y., Yap, C. C., Aizaki, H., Matsuura, Y., and Miyamura, T. (1999) Expression of hepatitis C virus NS5B protein: Characterization of its RNA polymerase activity and RNA binding, *Hepatology 29* (4), 1227−1235.
38. Watashi, K., Ishii, N., Hijikata, M., Inoue, D., Murata, T., Miyanari, Y., and Shimotohno, K. (2005) Cyclophilin B Is a Functional Regulator of Hepatitis C Virus RNA Polymerase, *Mol. Cell 19* (1), 111−122.
39. Zhong, W., Uss, A. S., Ferrari, E., Lau, J. Y., and Hong, Z. (2000) De novo initiation of RNA synthesis by hepatitis C virus nonstructural protein 5B polymerase, *J. Virol. 74* (4), 2017−2022.
40. Kao, C. C., Yang, X., Kline, A., Wang, Q. M., Barket, D., and Heinz, B. A. (2000) Template requirements for RNA synthesis by a recombinant hepatitis C virus RNA-dependent RNA polymerase, *J. Virol. 74* (23), 11121−11128.
41. Luo, G., Hamatake, R. K., Mathis, D. M., Racela, J., Rigat, K. L., Lemm, J., and Colonno, R. J. (2000) De novo initiation of RNA synthesis by the RNA-dependent RNA polymerase (NS5B) of hepatitis C virus, *J. Virol. 74* (2), 851−863.
42. Ranjith-Kumar, C. T., Kim, Y. C., Gutshall, L., Silverman, C., Khandekar, S., Sarisky, R. T., and Kao, C. C. (2002) Requirements for de novo initiation of RNA synthesis by recombinant flaviviral RNA-dependent RNA polymerases, *J. Virol. 76* (24), 12513−12525.
43. Zhong, W., Ingravallo, P., Wright-Minogue, J., Uss, A. S., Skelton, A., Ferrari, E., Lau, J. Y., and Hong, Z. (2000) RNA-dependent RNA polymerase activity encoded by GB virus-B non-structural protein 5B, *J. Viral Hepatol. 7* (5), 335−342.
44. Choi, K. H., Groarke, J. M., Young, D. C., Kuhn, R. J., Smith, J. L., Pevear, D. C., and Rossmann, M. G. (2004) The structure of the RNA-dependent RNA polymerase from bovine viral diarrhea virus establishes the role of GTP in de novo initiation, *Proc. Natl. Acad. Sci. U.S.A. 101* (13), 4425−4430.
45. Lévêque, V. J. P., Johnson, R. B., Parsons, S., Ren, J., Xie, C., Zhang, F., and Wang, Q. M. (2003) Identification of a C-Terminal Regulatory Motif in Hepatitis C Virus RNA-Dependent RNA Polymerase: Structural and Biochemical Analysis, *J. Virol. 77* (16), 9020−9028.

BI060511J